Carbohydrate Polymers 77 (2009) 851–857

Contents lists available at ScienceDirect

Carbohydrate Polymers

journal homepage: www.elsevier.com/locate/carbpol

Vibrational spectroscopy and X-ray diffraction methods to establish the differences between hardwood and softwood

Carmen-Mihaela Popescu [a,*], Ghita Singurel [b], Maria-Cristina Popescu [a], Cornelia Vasile [a], Dimitris S. Argyropoulos [c], Stefan Willför [d]

[a] Romanian Academy "P.Poni" Institute of Macromolecular Chemistry, 41A Gr. Ghica Voda Alley, RO-700487 Iaşi, Romania
[b] "Al. I.Cuza" University, Faculty of Physics, Optics and Spectroscopy Department, 11 Blvd. Carol I, Iaşi, Romania
[c] Organic Chemistry of Wood Components Laboratory, Department of Forest Biomaterials Science & Engineering, North Carolina State University, United States
[d] Process Chemistry Centre, Åbo Akademi University, Turku, Finland

ARTICLE INFO

Article history:
Received 23 January 2009
Received in revised form 26 February 2009
Accepted 2 March 2009
Available online 11 March 2009

Keywords:
FT-IR spectrometry
X-ray diffraction
Hardwood
Softwood

ABSTRACT

FT-IR spectrometry and X-ray diffraction were applied to probe the differences between pulp fibers from Eucalyptus wood (hardwood) and Norway spruce wood (softwood). Wood processing was found to induce certain structural alterations within its components depending on the type of wood and the applied procedure. These differences were established by using techniques such as; spectral comparison of wood samples with those of individual component fractions, derivative spectroscopy, bands deconvolution, etc. FT-IR spectroscopy was shown to be an important tool that provided details about the structural characteristics of hardwood and softwood samples. Using second-derivative spectra and deconvolution processes small differences between spectra became apparent that allowed correlations to be made related to wood composition. In addition a correlation was established between the integral absorptions for the various bands and lignin content as well as the lignin/carbohydrate content. Relations between various spectral characteristics and the degree of crystallinity and sample composition were established.

1. Introduction

Wood consists of an orderly arrangement of cells with cell walls composed of varying amounts of cellulose, hemicelluloses, and lignin. The great diversity of woody plants is reflected in their varied morphology and chemical composition. Typically, two general groups, hardwoods (angiosperms) and softwoods (gymnosperms) can be easily distinguished. Hardwoods have pores or vessel elements that occur among fiber and parenchyma cells. It is well-known that the cellulose content ranges from 40 to 50 wt% and the lignin content is comprised between 15 and 25 wt%, while that of the hemicelluloses varies from 15 to 25 wt%. Softwoods are composed of overlapping tracheids, connected by bordered pit apertures, and parenchyma cells and, in some cases, resin canals. Greater concentrations of lignin, about 5–10% more than in hardwoods, are found in softwoods, and about the same amount of cellulose 40–50%. Less hemicelluloses may be found in softwoods than hardwoods. The chemical composition of softwoods is also different from hardwoods with different types of lignin (primarily guaiacyl propane units), hemicelluloses (mannose is the most common constituent) and wood extractives (different terpenes, fatty acids, etc.). Differences in composition are also common between temperate and tropical hardwoods. Woods such as teak, mahogany and ebony have greater concentrations of lignin and wood extractives than many temperate hardwoods such as maple, birch, and aspen (Blanchette, Haight, Koestler, Hatcheld, & Arnold, 1994).

Cellulose is the dominant polymer in the biosphere. It is an optically anisotropic system being made up of poly-(1 → 4)-β-D-glucose chains (Atalla, 1999; O'Sullivan, 1997).

The numerous polar groups make cellulose molecules predestined for building up hydrogen bonds within the molecule and between the different molecules. In the generally accepted structure of cellulose I, intramolecular hydrogen bonds of types 3-OH···O-5 and 2-OH···O-6 are present for both sides of the chain. As a result of hydroxyl groups showing different polarities, cellulose has different crystalline structures, ranging from cellulose I (native cellulose) to cellulose IV. Moreover, cellulose I is itself composed of two different crystalline forms: cellulose Iα and Iβ. Two chains, which take an almost fully extended conformation, are contained in the unit cell of cellulose I. It is generally known and accepted that the hydrogen bonds play an important role in the conformational and mechanical properties of cellulosic materials (O'Sullivan, 1997).

Besides its complex crystalline structure, native cellulose also has a complex arrangement within the wood fiber wall. In the

* Corresponding author. Tel.: +40 232217454; fax: +40 232211299.
E-mail address: mihapop@icmpp.ro (C.-M. Popescu).

0144-8617/$ - see front matter © 2009 Elsevier Ltd. All rights reserved.
doi:10.1016/j.carbpol.2009.03.011

secondary wall, the cellulose chains are grouped into fibrils by hydrogen bonds. These fibrils are aligned in different directions in the different secondary wall layers.

Infrared spectroscopy, which is known to be sensitive to structural features, has had a long tradition in wood research. Since the very first use of infrared spectroscopy to elucidate molecular structures, much effort has been devoted to separating the overlapping bands deriving, for example, from hydrogen bonds (Fengel & Ludwig, 1991; Nishiyama, Isogai, Okano, Müller, & Chanzy, 1999; Sugiyama, Persson, & Chanzy, 1991; Tashiro & Kobayashi, 1991).

General difficulties in wood and pulp analyses principally arise from the numerous components with different chemical character. The extractives of wood and pulp cover a wide range of low-molar-mass compounds, which may be isolated for a detailed chemical examination by means of different solvent extractions. The isolation of lignin from wood and pulp samples in its unaltered form at an acceptable and representative yield is currently a major problem, despite a variety of versatile extraction schemes that have been proposed. However, recently a new method of lignin isolation termed enzymatic mild acidolysis lignin (EMAL) promises to alleviate these problems, This method has actually been applied to the samples examined in this work (Guerra, Filpponen, Lucia, & Argyropoulos, 2006b; Guerra et al., 2006a; Popescu et al., 2006; Wu & Argyropoulos, 2003). Determination of the carbohydrate composition of wood and pulp samples is vital for many applications and is one of the most frequently performed chemical analyses for almost all biomass-derived materials. Elaboration of a procedure to analyse direct the differences between various kinds of wood samples is necessary.

The aim of this paper is to establish the main structural and morphological differences between hardwood and softwood samples. FT-IR spectrometry and X-ray diffraction have been used. Optimum experimental conditions were initially established for each method and differences between the various samples were assessed by assignment of the characteristic bands, evaluation integral absorption or carbohydrate/lignin ratio, etc., from FT-IR spectra and percentage of crystalline fraction by X-ray diffraction. The accumulated data were finally discussed in terms of sample composition.

2. Experimental

2.1. Materials

The unfractioned samples of unbleached Kraft pulp brown stock (BSP) of *Eucalyptus globulus* (sampled after washing stages) and unbleached Norway spruce TMP (sampled in a Swedish mill, ca. 38% dryness, 85 ml CSF, standard newspaper quality, the mill has one-stage refining and a subsequent reject refining (ca. 20%) stage) were provided by Åbo Akademi University, Laboratory of Wood and Paper Chemistry, Turku, Finland. The samples were part of the COST Action E41 joint analytical effort on wood and its components.

Different working groups (WG1, WG2 and WG3 constituted of different laboratories partners) of COST Action E41 Project, determined the composition of the wood components following different separation procedures. The results were summarized at Grenoble Meeting (April 12–13, 2006). The average content of the various components are shown in Table 1.

The selected samples for study have very different contents in extractives, carbohydrates and lignins. Eucalyptus BSP has ~20 wt% more carbohydrates that Norway spruce, while lignin content is very small of 1–1.7 wt% and very high of 27–29 wt% in Norway spruce pulp. Unbleached pulps were studied.

Isolation of enzymatic mild acidolysis ligins (EMALs): These were isolated form Eucalyptus chips (*Eucalyptus globulus*) and from Norway spruce TMP. The wood chips, or TMP fibers, were ground to pass a 20-mesh screen in a Wiley mill and Soxhlet extracted with acetone for 48 h. The resulting Wiley-milled wood powder was air-dried and stored in a desiccator under vacuum. The *E. globulus* wood powder was submitted to an alkaline extraction with 0.3% (0.075 mol L^{-1}) NaOH for 1 h to remove tannins before use (Evtuguin et al., 2001).

Table 1
Average contents of total extractives, carbohydrates and lignin in *Eucalyptus globulus* and Norway spruce pulps.

Samples	Extractives[a] (wt%)	Carbohydrates[b] (wt%)	Lignin[c] (wt%)
Eucalyptus BSP	0.2	88.7–99.2	1.0–1.7
Norway spruce TMP	1.0	60.6–69.0	27.6–29.4

[a] Total average amounts determined by acetone extraction [15] (Willför, Hemming, & Leppänen, 2006).
[b] Total amounts determined by HPAEC-PAD [16] (Puls, 2006).
[c] Total amounts (ASL + AIL) [17] (de Jong, 2006).

Rotary ball milling was performed in a 5.5 L porcelain jar in the presence of 474 porcelain balls (9.4 mm of diameter), which occupied 18% of the active jar volume. One hundred grams of extractive-free wood powder was loaded into the jar, creating a porcelain ball/wood weight ratio of 16.6. The milling process was conducted at room temperature for up to 28 days with a rotation speed of 60 rpm (Guerra et al., 2006a). EMALs were isolated from ball milled wood according to the procedure described by Wu and Argyropoulos (2003). Some cautions to avoid contamination in the final product were taken into account, as previously reported (Guerra et al., 2006a).

2.2. Characterisation methods

The methods of investigation in this work were FT-IR spectroscopy and X-ray diffraction.

FT-IR spectra were recorded on solid samples in KBr pellets by means of an FT-IR Bomem MB-104 spectrometer (Canada) with a resolution of 4 cm^{-1}. The concentration of the samples in the pellets was constant of 5 mg/500 mg KBr. Samples were sieved and fractionated. The fraction with grains having diameter less than 0.2 mm was retained for analysis. Five recordings were performed for each sample after successive milling and the evaluations were made on the average spectrum obtained from these five recordings. Processing of the spectra was done by means of Grams/32 program (Galactic Industry Corp.). Each method yielded several components. For a better understanding of the structure of the samples, deconvolution of the spectra was carried out with Gaussian profiles. The number and the maximum of the deconvoluted peaks were taken from second-derivative spectra. The reduced chi-squared value for all the deconvoluted curves was $\chi^2 \leqslant 0.1$; therefore, the use of this function is a good approach.

The X-ray diffractograms were recorded on XRD equipment Rigaku RINT 2500/32 by Rigaku Co. Japan. The measurements were carried out in point focus geometry using CuKα radiation $\lambda = 0.1524$ nm. Experimental conditions: sequence scan mode; measuring axis: 2θ; voltage: 40 kV; current: 20 mA; start angle: 10°; stop angle: 80°; sampling angle: 0.021°; scan rate of goniometer: 2°/min; divergent slit width: 1°; receiving slit width: 1°; scattering slit width: 0.60 mm; monochromator receiving slit width: 0.80 mm. All the measurements were conducted in the diffraction mode at atmospheric pressure.

The diffractograms were deconvoluted using Gaussian and mixed Gaussian–Lorentzian profiles. The reduced chi-squared value for all the deconvoluted curves was $\chi^2 \leqslant 0.1$; therefore, the use of this function is a good approach. The fitting curve matches the experimental curve very well. After deconvolution, the several parameters can be calculated and compared (He, Tang, & Wang,

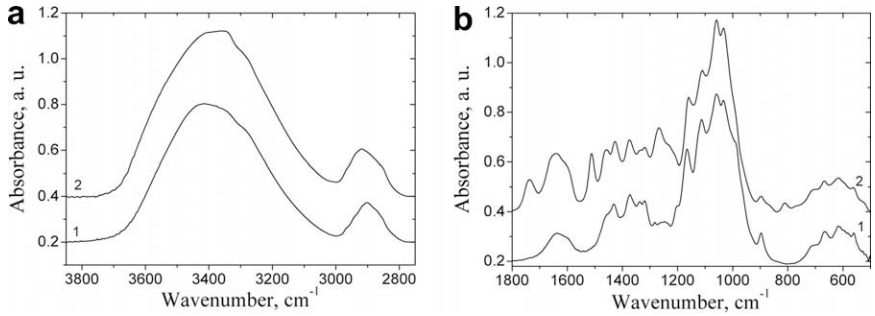

Fig. 1. FT-IR spectra of the 3700–2700 cm^{-1} (a) and 1850–500 cm^{-1} (b) regions for: Eucalyptus BSP (1), Norway spruce TMP pulp (2) samples.

2007; Heinze & Liebert, 2001) e.g. the crystalline index; apparent crystallite size, proportion of crystallite interior chains; orientation index; mesomorphism and mass fraction of cellulose in wood.

3. Results and discussion

3.1. FT-IR spectroscopy

Two information-rich regions of the FT-IR spectra namely, 3800–2800 cm^{-1} and 1800–600 cm^{-1}, of the studied samples are shown in Fig. 1a and b.

The main bands are assigned to asymmetric methoxyl C—H stretching at 2916 cm^{-1}, absorbed water at 1637 cm^{-1}, bands assigned to different lignin groups, such as: 1737, 1594, 1510, 1263, and 1130 cm^{-1}, bands common to lignin and cellulose such as: 1455, 1427, 1373, 1338, 1234, 1166, 1111, and 1029 cm^{-1} and bands assigned to cellulose such as: 1317, 1283, and 1060 cm^{-1}. In the "fingerprint" region some bands which are assigned to lignin were not found (1737 cm^{-1}) or their integral absorptions were very low (1594, 1510, and 1263 cm^{-1}) in Eucalyptus BSP sample, while in the spectra of Norway spruce TMP these bands are present and the integral absorption is quit high.

For a good differentiation of the bands the second derivative of the spectra was made. Generally, the secondary derivative of IR spectra can obviously enhance the apparent resolution and amplify small differences of IR spectrum. These were obtained with the Savitsky–Golay method (second-order polynomial with fifteen data points) using Grams 32 program. The second-derivative spectra of the samples are shown in Fig. 2.

From the derivative FT-IR spectra of the samples several differences can be observed. The bands at 1737, 1637, 1596, 1510, and 1455 cm^{-1} are very weak in the Eucalyptus BSP sample while in Norway spruce TMP they are well evidenced; the bands at 1268, 1229, 1209, 1059, and 1022 cm^{-1} appear more prominent and are more apparent in the Norway spruce TMP sample.

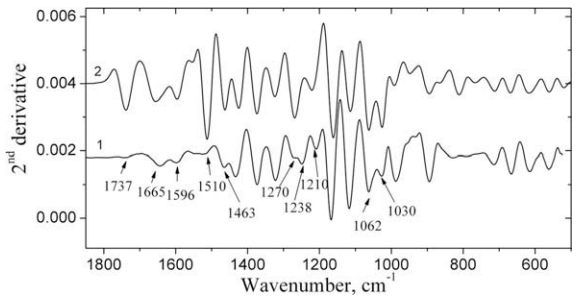

Fig. 2. Second derivative of FT-IR spectra in the "fingerprint" region (1850–900 cm^{-1}) for: Eucalyptus BSP (1) Norway spruce TMP pulp (2) samples.

Deconvolutions of the 3800–2750 cm^{-1}, 1850–1550 cm^{-1}, 1550–1250 cm^{-1}, and 1250–900 cm^{-1} regions for FT-IR spectra were made. After these was possible to evaluate the integral absorptions and the height of each band. In Fig. 3a–h the deconvolutions spectra of the Eucalyptus BSP and Norway spruce TMP samples are shown.

In the 3800–2750 cm^{-1} region (Fig. 3a and b) both samples shows seven bands, such as: 3561, 3419, 3344, 3277, 3111, 2916, and 2854 cm^{-1}, but the absorbances of the main bands are different as well as their positions.

The most representative bands in the 3800–2700 cm^{-1} are those assigned to —OH intramolecular and intermolecular stretching modes (3567, 3423, 3342, 3278, and 3106 cm^{-1}), to asymmetric and symmetric methyl and methylene stretching (2921 and 2854 cm^{-1}) presented in the spectra of all components of wood but especially in the spectra of cellulose.

As the main bands are assigned to various hydroxyl groups, absorbed water and hydrogen bonds, they are more pronounced in Eucalyptus BSP spectrum because of high content of cellulose whose functional groups readily interact inter- and intramolecularly.

The "fingerprint" region 1800–800 cm^{-1} (Fig. 3e–h) is complicated and a complex one. It is comprised of 27 bands, some of them being evident only by deconvolution.

The deconvoluted spectra in all examined regions are different between Eucalyptus BSP and Norway spruce TMP samples. Generally in the Eucalyptus BSP spectrum, the bands assigned to lignin (1594, 1510, and 1263 cm^{-1} assigned to C=C stretching of the aromatic ring and C—O stretch in lignin, respectively) present very low absorption intensities or even are missing (1737 cm^{-1} assigned to C—O stretch in unconjugated ketones). This is due to the fact that the content of lignin in this sample is very low (~2 wt% by chemical determination (Pakkanen, 2006)), while in the Norway spruce TMP sample the content of lignin is quit high (~28.4% by chemical determination (Pakkanen, 2006)) – Table 1.

In the 3800–2700 cm^{-1} region, four bands assigned to different hydrogen bonded —OH vibrations were found. For these bands were calculated the energy of hydrogen bonds and hydrogen bonding distance.

The energy of the hydrogen bonds was calculated using equation (Struszczyk, 1986):

$$E_H = \frac{1}{k}\left[\frac{(v_0 - v)}{v_0}\right] \quad (1)$$

where $v_0 \rightarrow$ standard frequency corresponding to free —OH groups (3650 cm^{-1}), $v \rightarrow$ the frequency of the bonded —OH groups, and $k \rightarrow$ is a constant equal with 2.61 * 10^{-2} kJ^{-1}.

The calculated energy of hydrogen bonds – Table 2 – represents a small decrease for Norway spruce TMP in respect with Eucalyptus BSP. This could be explained by high content of cellulose and its ordering which create stronger hydrogen bonds in the Eucalyptus

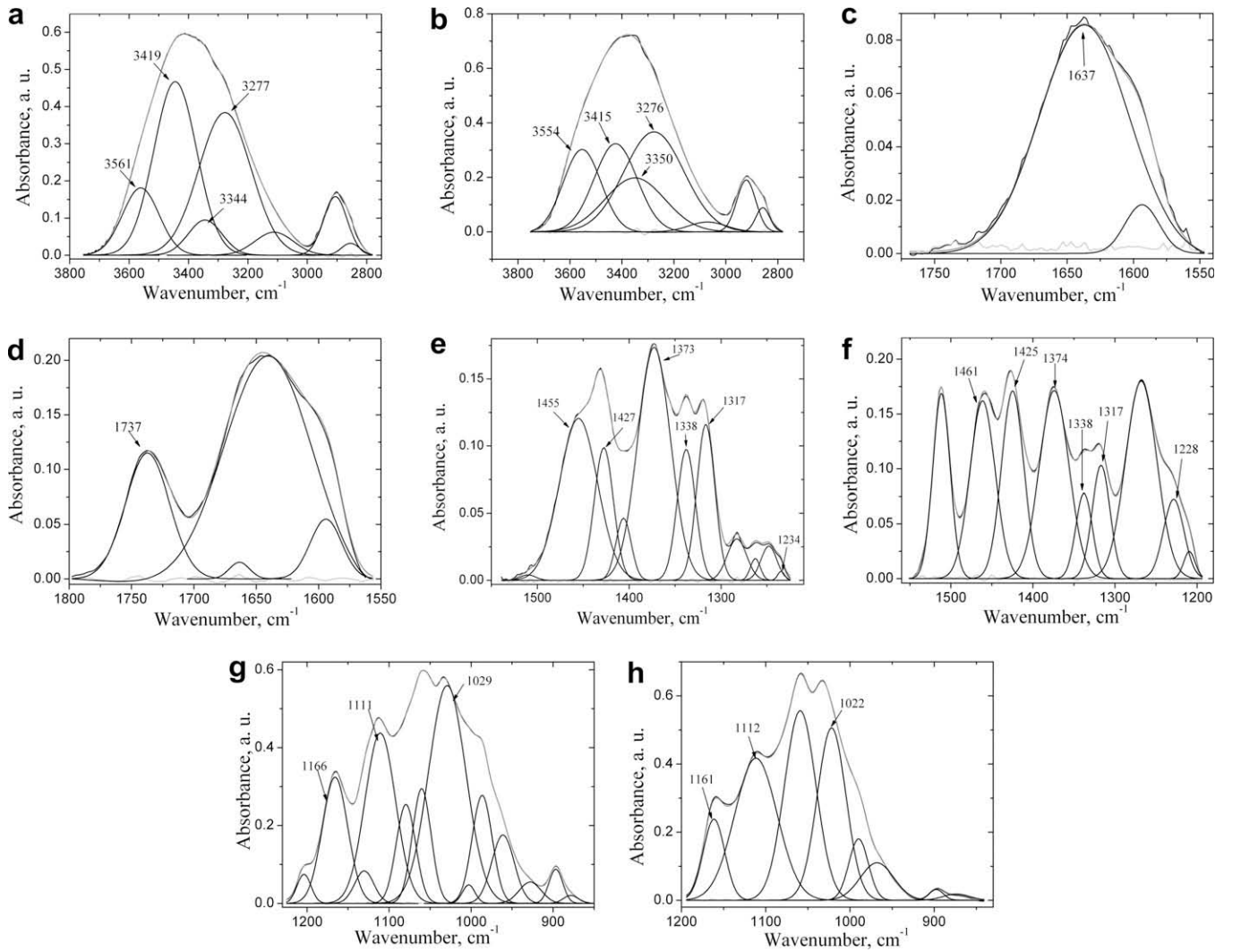

Fig. 3. The deconvoluted spectra of four different spectral regions 3800–2700 cm^{-1}, 1800–1550 cm^{-1}, 1550–1250 cm^{-1}, and 1250–900 cm^{-1} regions for Eucalyptus BSP (a, c, e, and g) and Norway spruce TMP (b, d, f, and h) samples.

BSP sample while in the Norway spruce TMP sample because of the composition (lower cellulose content) and structure of softwood these interactions are not so strong like in the hardwood sample. Only the energy for the free OH (6) and OH (2), weakly absorbed water is increasing in Norway spruce TMP in respect with Eucalyptus BSP. This can be due to the structure of the softwood which has many irregularities and the water desorption is easier.

The hydrogen bonding distances are obtained by using the Sederholm equation (Pimentel & Sederholm, 1956):

$$\Delta v(\mathrm{cm}^{-1}) = 4.43 * 10^3(2.84 - R) \quad (2)$$

where $\Delta v = v_0 - v$

$v_0 \rightarrow$ monomeric —OH stretching frequency, is taken to be 3600 cm^{-1}, $v \rightarrow$ stretching frequency observed in the infrared spectrum of the sample (Wan & Kuo, 2001).

The hydrogen bonding distances – Table 3 – are similar for both kinds of studied wood samples.

In the "fingerprint" region the spectra are very complex containing many bands assigned to main wood components. These are positioned at: 1594, 1510, 1268, and 1130 cm^{-1} and are assigned to characteristic bending or stretching of different groups from lignin, while the bands centred at 1455, 1427, 1373, 1338, 1234, 1166, 1111, and 1029 cm^{-1} assigned to characteristic bending or stretching vibrations of different groups commonly for lignin and cellulose, and finally the bands at 1737, 1317, 1283, 1166, and 1060 cm^{-1} are assigned to characteristic bending or stretching vibrations of the different groups from cellulose.

In the spectrum of the Eucalyptus BSP sample, some bands assigned to characteristic bending or stretching for different lignin groups are missing (1737 cm^{-1}) or are very small (1510, 1268,

Table 2
The energy of the hydrogen bonds for studied samples.

Samples	Hydrogen bonding energy (E_H) (kJ/mol)			
	3561 cm^{-1}	3422 cm^{-1}	3348 cm^{-1}	3277 cm^{-1}
Eucalyptus BSP	6.364	16.518	21.881	26.672
Norway spruce TMP	6.865	16.303	21.595	26.743

Table 3
The hydrogen bonding distance for studied samples.

Samples	Hydrogen bonding distance (R) (Å)			
	3567 cm^{-1}	3432 cm^{-1}	3342 cm^{-1}	3252 cm^{-1}
Eucalyptus BSP	2.83	2.80	2.78	2.77
Norway spruce TMP	2.83	2.80	2.78	2.76

and 1234 cm^{-1}) in comparison with the same bands in the Norway spruce TMP sample. This later group of bands in the first sample was possible to detect only after deconvolution. The integral absorption of the bands assigned to characteristic bending or stretching in lignin groups increases strongly for the Norway spruce TMP sample in comparison with the same bands form the spectrum of the Eucalyptus BSP sample – Fig. 4. Only for bands at 1594 cm^{-1} assigned to C=C stretching of the aromatic ring (S), C=O stretch, CH deformation, and 1130 cm^{-1} assigned to aromatic C—H in plane deformation; typical for G units, whereby G condensed >G etherified the increase is not so readily apparent.

The variation of the integral absorptions of the IR bands, assigned to characteristic bending or stretching vibrations of different groups from cellulose (1317 cm^{-1} assigned to CH_2 wagging in cellulose I and cellulose II and 1166 cm^{-1} assigned to C—O—C asymmetric stretching in cellulose I and cellulose II) – Fig. 5 – are the highest in Eucalyptus BSP than in Norway spruce TMP sample. In the same time the bands at 1283 cm^{-1} (assigned to CH bending in cellulose I and cellulose II) and at 1066 cm^{-1} (assigned to C—O valence vibration mainly from C(3)—O(3)H) varies in opposite direction. This is due to a greater amount of cellulose groups.

The integral absorption bands which are assigned to characteristic bending or stretching vibrations commonly for lignin and cellulose present a small decrease from the spectra of Eucalyptus BSP to Norway spruce TMP sample (see Fig. 6).

The spectral differences found are in accordance with chemical composition determined by other methods (Pakkanen, 2006).

In this group, the bands at 1455 cm^{-1} assigned to C—H asymmetric deformation in CH_2 and CH_3 from methoxyl group, 1427 cm^{-1} assigned to C—H asymmetric deformation in —OCH_3, H—O—C in plane bending of alcohol groups in cellulose, 1373 cm^{-1} assigned to symmetric C—H bending from —OCH_3, O—H, and C—O of phenol and tertiary alcohol, CH bending in cellulose I and cellulose II and 1234 cm^{-1} assigned to syringyl ring breathing with C—O stretching, C—C stretching, OH in plane deformation, present a small increase for Norway spruce TMP in respect with Eucalyptus BSP. This is due to a greater amount of lignin in the Norway spruce TMP sample.

The intensities of several IR absorption bands, characteristic for cellulose, were also compared to the intensity of the 1510 cm^{-1} band that is sometimes used as an internal standard assigned to benzene ring stretching vibration for lignin (see Table 4).

The relation between lignin and carbohydrates can be calculated by the ratio of some bands of the FT-IR spectra. As it is expected the lignin/carbohydrate ratios are very high in Norway spruce TMP compared to Eucalyptus BSP, as is evident from the increase of the 1510 cm^{-1} band assigned to lignin.

For a good characterisation of the Eucalyptus BSP and Norway spruce TMP samples, FT-IR spectra of the fractions obtained by successive extractions were also examined. Fig. 7 shows the "fingerprint" region of FT-IR spectra for the acetone extractive for Eucalyptus BSP and Norway spruce TMP samples.

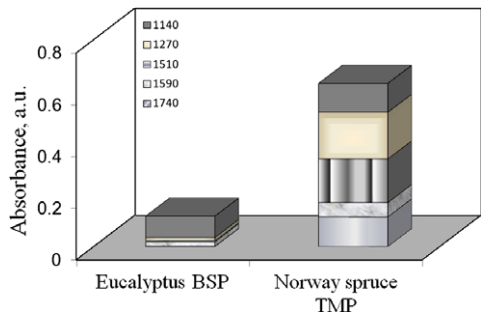

Fig. 4. The variations of the integral absorption of the lignin representative bands from the Eucalyptus BSP and Norway spruce TMP samples spectra.

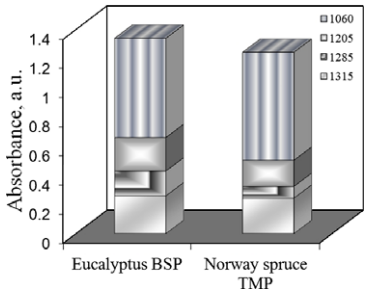

Fig. 5. The variations of the integral absorption of the cellulose representative bands from the Eucalyptus BSP and Norway spruce TMP samples spectra.

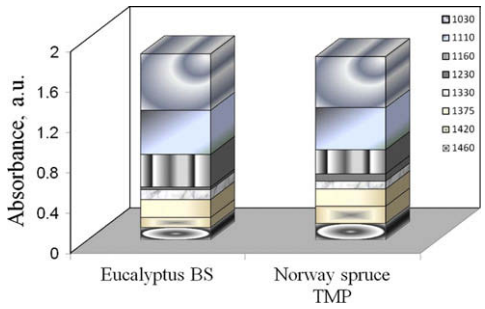

Fig. 6. The variations of the integral absorption of the lignin and cellulose common representative bands from the Eucalyptus BSP and Norway spruce TMP samples spectra.

By chemical determinations, the amounts of acetone extractives in samples are: 0.2 wt% for Eucalyptus BSP and 1.0 wt% for Norway spruce TMP sample. The differences, which appear in the IR spectra of the samples, are due to the fact that some extractives (resin acids, lignans, and triglycerides), are not detected or the detected amount is very low. In addition, all determined extractives amounts are lower in the Eucalyptus BSP sample, than in the Norway spruce TMP sample (Wan & Kuo, 2001).

The acetone extractives spectra show some differences in the 1650–1500 cm^{-1} and 1200–900 cm^{-1} regions. For example in the Eucalyptus BSP spectrum, the band at 1594 cm^{-1} assigned to C=O stretch and CH deformations, is present as a shoulder while in the other spectrum is more evident. The band at 1510 cm^{-1} assigned to C—H deformations, is evident in normal spectra of the Norway spruce TMP sample, while in the Eucalyptus BSP sample was only possible to be detected by second-derivative spectra and deconvolution. For the Norway spruce TMP sample the band at 1161 cm^{-1} assigned to C—H in plane deformations is observable as a shoulder, while for the Eucalyptus BSP sample this band was only possible to be detected by second-derivative spectra and deconvolution.

Also the intensity of the band at 1072 cm^{-1} assigned to C—O deformation of secondary alcohols and aliphatic ethers, is increas-

Table 4
Lignin/carbohydrate ratio calculated from FT-IR spectra.

Sample	I_{1510}/I_{1375}	I_{1510}/I_{1158}	I_{1510}/I_{895}	L/C[a]
Eucalyptus BSP	0.023	0.012	0.045	0.017
Norway spruce TMP	0.988	0.707	1.836	0.420

[a] L/C (lignin/cellulose content chemically determined) ratio using the highest values of total amount from Table 1.

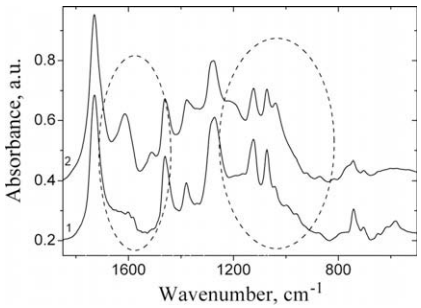

Fig. 7. FT-IR spectra of the acetone extractives of: Eucalyptus BSP (1) and Norway spruce TMP pulp (2) samples.

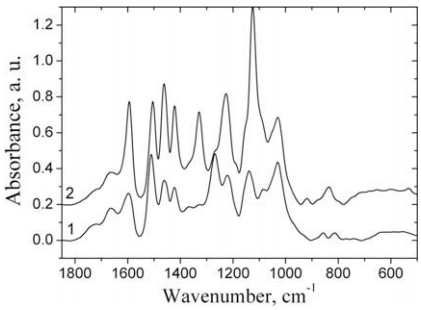

Fig. 8. FT-IR spectra of the lignin samples: enzymatic mild acidolysis Norway spruce (1), enzymatic mild acidolysis Eucalyptus chips (2).

ing in the Eucalyptus BSP sample, while the band at 1040 cm^{-1} assigned to C—C and C—O stretching is evident only as a shoulder. In the spectrum of the second sample these bands have almost the same intensity and are overlapped. The integral absorptions of the bands were determined by deconvolution. Therefore the extractives of the two samples are different in the 1650–1500 cm^{-1} and 1200–900 cm^{-1} regions. The band positions in the extractive spectra are overlapped with those assigned to different lignin or carbohydrate groups' vibrations. Probably because of their low content they actually influence only to a small extent the global FT-IR spectra.

The FT-IR spectra of EMAL lignins obtained by enzymatic mild acidolysis of Eucalyptus chips and enzymatic acidolysis of Norway spruce TMP samples are presented in Fig. 8.

The FT-IR spectra of the various lignin samples show, in the "fingerprint" region, the bands assigned to characteristic bending or stretching vibrations for the different specific lignin groups. Generally, the differences between samples are due to the structural differences of lignin, which are influenced by the type of wood and extraction method used for the separation process. The integral absorptions of the bands from enzymatic acidolysis Norway spruce (EMAL) lignin are lower than integral absorption of the bands from enzymatic mild acidolysis Eucalyptus (EMAL) lignin. The integral absorptions of the bands at 1595, 1460, 1422, 1365, 1324, 1219, and 1140 cm^{-1} are higher in the EMAL of Eucalyptus chips lignin than those of the EMAL of the Norway spruce chips lignin. These are due to a higher amount of β-aryl ether and aliphatic —OH functional groups in the EMAL Eucalyptus lignin sample than in EMAL Norway spruce lignin sample (Argyropoulos, 2006). The integral absorption of the bands at 1720 cm^{-1} assigned to C—O stretch in unconjugated ketones, carbonyls and in ester groups; C=O valence vibration of acetyl or COOH groups and 1270 cm^{-1} assigned to guaiacyl ring breathing, C—O stretch in lignin, C—O linkage in guaiacyl aromatic methoxyl groups are higher in the EMAL of the Norway spruce lignin than those of the EMAL of Eucalyptus lignin.

FT-IR spectroscopy gives us important details about the characteristic structure of such complex samples. Second-derivative spectra and the deconvolution process also play an important role. Using the spectral study, correlations were made between wood composition and the energy of the hydrogen bonds and hydrogen bonding distance and also between the integral absorptions of the bands and lignin content and the lignin/carbohydrate ratio, and also were observed differences which appear between different wood samples.

3.2. X-ray diffraction data

Fig. 9 shows the X-ray diffractograms of the Eucalyptus BSP and Norway spruce TMP samples. The X-ray peaks at $2\theta = 15°$ and 16.5° merged into a broad band, which is consistent with the literature accounts (Marcovich, Reboredo, & Aranguren, 2001; Newman, 1999). The most prominent peak was found to be at $2\theta = 22.4°$ and this was used in our subsequent calculations. This peak is assigned to (200) plane, which is not parallel to any plane. The X-ray diffraction pattern of wood is mainly that of cellulose.

In order to examine the intensities of diffraction bands and to establish the crystalline and the amorphous areas more precisely, the diffractograms were deconvoluted (Fig. 9).

The positions of the peaks responsible for the cellulose crystalline form I, were found not to be significantly different to that obtained for Eucalyptus BSP and Norway spruce TMP samples.

After deconvolution, five bands were observed, namely: the 15° (2θ) reflection assigned to the (101) crystallographic plane, the 16.5° (2θ) reflection, assigned to the $(10\bar{1})$ crystallographic plane, the 18.9° (2θ) reflection, assigned to amorphous phases, the 20.4° (2θ) reflection, assigned to the (012) crystallographic plane, and the 22.4° (2θ) reflection, assigned to the (002) or (200) crystallographic plane of cellulose I (Colom, Carrillo, Nogues, & Garriga, 2003; Donald & Astley, 2005; Heinze & Liebert, 2001; Marcovich et al., 2001). All peaks from the diffractogram are increasing in the Eucalyptus BSP sample when compared to the Norway spruce TMP sample.

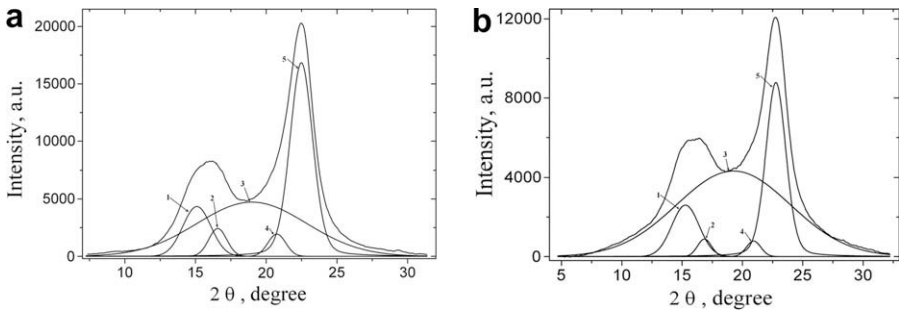

Fig. 9. Deconvoluted X-ray diffractograms of Eucalyptus BSP (a) and Norway spruce TMP pulp (b) samples (1 – 101 crystallographic plane; 2 – $10\bar{1}$ crystallographic plane; 3 – amorphous phases; 4 – 012 crystallographic plane; 5 – 002 or 200 crystallographic plane of cellulose I).

Table 5
The calculated values of several parameters estimated from the diffraction pattern for studied samples.

Parameter	Eucalyptus BSP	Norway spruce TMP
Cr.I.	0.543	0.384
Cr.I.′	0.690	0.506
L_{002} (nm)	3.504	2.944
X	0.455	0.375
O.I.	0.759	0.638
Mesomorphism	0.216	0.132
Cellulose content	0.978	0.548

Crucial for the analysis of the XRD data is the separation of the reflection (002) from the amorphous background and the reflections (012), (101), and $(10\bar{1})$.

In Table 5 the calculated parameters from X-ray diffractogram for the studied samples are presented.

The cellulose content found by X-ray is in accordance with that found by HPAEC-PAD, see Table 1.

The uncertainties in the crystallinity index determination are 3% ($N = 3$) and in the intensity ratio 4%. All calculated values of the estimated parameters are higher for the Eucalyptus BSP compared to the Norway spruce TMP sample. The elimination of the hemicelluloses and lignin created in appearance an increase in the crystalline order of cellulose in pulp sample. For the Eucalyptus BSP sample there is a large amount of cellulose ~98% and the diffraction pattern was not influenced by other components. In the case of Norway spruce TMP sample there is presented a higher amount of lignin, which is strongly connected together with hemicelluloses and cellulose components, and these can influence the X-ray diffraction pattern.

4. Conclusion

FT-IR spectroscopy and X-ray diffraction allow evidencing the differences which appear in structure of components between hardwood and softwood. The I_{1510}/I_{1375} ratio gives, with a good approximation, information about the lignin/carbohydrate ratio. The energy of hydrogen bonds of the softwood sample is lower and the hydrogen bonding distances are longer.

The crystallinity index is lower in softwood than in hardwood. It is seems that higher energy of hydrogen bonds increases the crystallinity degree.

In hardwood, there are bands assigned to syringyl units with higher integral absorptions than in softwood, while the bands assigned to guaiacyl units vary inversely.

Acknowledgements

This work was carried out under the COST E41 project: Analytical Tools with Applications for Wood and Pulping Chemistry (http://KCL.FI/COST/index.html).

References

Argyropoulos, D. S. (2006). Yield, functional groups & molecular weights for Cost E41 lignins, In *Proceedings of the COST E41 meeting: Progress of the "COST Action E41 Joint Analysis Effort" on wood and fiber characterisation*, Grenoble, France, April 12–13.

Atalla, R. H. (1999). Celluloses. In D. Barton, K. Nakanishi, & O. Meth-Cohn (Eds.), *Comprehensive natural products chemistry* (pp. 529–543). Oxford: Elsevier Science.

Blanchette, R. A., Haight, J. E., Koestler, R. J., Hatcheld, P. B., & Arnold, D. (1994). Assessment of deterioration in archaeological wood from ancient Egypt. *Journal of the American Institute for Conservation, 33*, 55–70.

Colom, X., Carrillo, F., Nogues, F., & Garriga, P. (2003). Structural analysis of photodegraded wood by means of FTIR spectroscopy. *Polymer Degradation and Stability, 80*, 543–549.

de Jong, E. (2006). Compositional characterisation of wood and pulps: Summary WG1, In *Proceedings of the COST E41 meeting, progress of the "COST Action E41 Joint Analysis effort" on wood and fiber characterisation*, Grenoble, France, April 12–13.

Donald, A. M., Astley, O .M. (2005). Available via DIALOG www.ccp13.ac.uk/fdr/2001/html/pdf/print/19.pdf Accessed 18. 08.05.

Evtuguin, D., Neto, C., Silva, A., Domingues, P., Amado, F., Robert, D., et al. (2001). Comprehensive study on the chemical structure of dioxane lignin from plantation *Eucalyptus globulus* wood. *Journal of Agricultural and Food Chemistry, 49*, 4252–4261.

Fengel, D., & Ludwig, M. (1991). Possibilities and limits of the FTIR spectroscopy for the characterization of cellulose. *Papier, 45*, 45–51.

Guerra, A., Filpponen, I., Lucia, L., Saquing, C., Baumberger, S., & Argyropoulos, D. S. (2006a). Toward a better understanding of the lignin isolation process from wood. *Journal Agricultural and Food Chemistry, 54*, 5939–5947.

Guerra, A., Filpponen, I., Lucia, L., & Argyropoulos, D. S. (2006b). Comparative evaluation of three lignin isolation protocols for various wood species. *Journal Agricultural and Food Chemistry, 54*, 9696–9705.

He, J., Tang, Y., & Wang, S.-Y. (2007). Differences in morphological characteristics of bamboo fibres and other natural cellulose fibres: Studies on X-ray diffraction, solid state ^{13}C-CP/MAS NMR, and second derivative FTIR spectroscopy data. *Iranian Polymer Journal, 16*, 807–818.

Heinze, T., & Liebert, T. (2001). Unconventional methods in cellulose functionalization. *Progress in Polymer Science, 26*, 1689–1762.

Marcovich, N. E., Reboredo, M. M., & Aranguren, M. I. (2001). Modified woodflour as thermoset fillers. II. Thermal degradation of woodflours and composites. *Thermochimica Acta, 372*, 45–57.

Newman, R. H. (1999). Estimation of the lateral dimensions of cellulose crystallites using ^{13}C NMR signal strengths. *Solid State Nuclear Magnetic Resonance, 15*, 21–29.

Nishiyama, Y., Isogai, A., Okano, T., Müller, M., & Chanzy, H. (1999). Intracrystalline deuteration of native cellulose. *Macromolecules, 32*, 2078–2081.

O'Sullivan, A. C. (1997). Cellulose: The structure slowly unravels. *Cellulose, 4*, 173–207.

Pakkanen, H. (2006). Chemical composition of the COST E41 integration samples analyses by standard methods, In *Proceedings of the COST E41 meeting: Progress of the "COST Action E41 Joint Analysis Effort" on wood and fiber characterisation*, Grenoble, France, April 12–13.

Pimentel, G. C., & Sederholm, C. H. (1956). Correlation of infrared stretching frequencies and hydrogen bond distances in crystals. *Journal of Chemical Physics, 24*, 639–641.

Popescu, C.-M., Vasile, C., Popescu, M.-C., Singurel, Gh., Popa, V. I., & Munteanu, B. S. (2006). Analytical methods for lignin characterization. II. Spectroscopic studies. *Cellulose Chemistry and Technology, 40*, 597–621.

Puls, J. (2006). Summary of WG2 results, In *Proceedings of the COST E41 meeting: Progress of the "COST Action E41 Joint Analysis Effort" on wood and fiber characterisation*, Grenoble, France, April 12–13.

Struszczyk, H. (1986). Modification of lignins. III. Reaction of lignosulfonates with chlorophosphazenes. *Journal of Macromolecular Science A, 23*, 973–992.

Sugiyama, J., Persson, J., & Chanzy, H. (1991). Combined infrared and electron diffraction study of the polymorphism of native celluloses. *Macromolecules, 24*, 2461–2466.

Tashiro, K., & Kobayashi, M. (1991). Theoretical evaluation of three-dimensional elastic constants of native and regenerated celluloses: Role of hydrogen bonds. *Polymer, 32*, 1516–1526.

Wan, C.-H., & Kuo, J.-F. (2001). Infrared spectroscopic and mesomorphic studies of 4,4′-bis(?-hydroxyalkoxy)-a-methylstilbenes. *Liquid Crystals, 28*, 535–548.

Willför, S., Hemming, J., Leppänen, A.-S. (2006). Analysis of extractives in different pulps – Method development, evaluation, and recommendations. *Report B1-06*, Åbo Akademi University, Process Chemistry Centre, Laboratory of Wood and Paper Chemistry, Åbo (ISSN 1796-6086, ISBN 952-12-1783-9).

Wu, S., & Argyropoulos, D. S. (2003). An improved method for isolating lignin in high yield and purity. *Journal of Pulp and Paper Science, 29*, 235–240.